

Supplemental Information

Worry and FRET: ROS Production Leads to Fluorochrome Tandem Degradation and impairs Interpretation of Flow Cytometric Results

Isaac J. Jensen, Patrick W. McGonagill, Mitchell N. Lefebvre, Thomas S. Griffith, John T. Harty, and Vladimir P. Badovinac

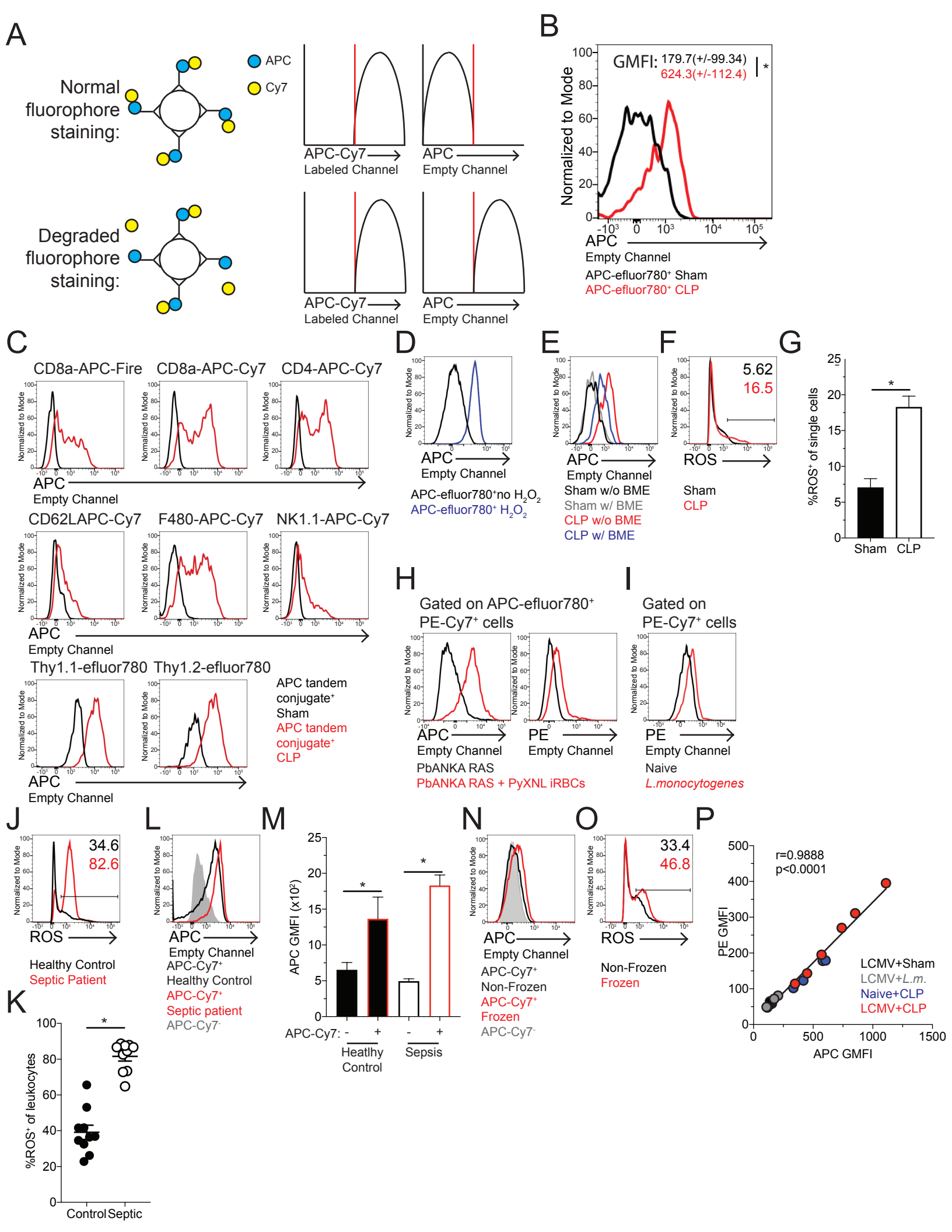


Figure S1. Differential Tandem Fluorophore Degradation between Experimental Groups and/or Samples Obscures Interpretation of Flow Cytometric Data

A) In an ideal system, tandem conjugate fluorophores would not degrade and only fluoresce in their given channel without fluorescing in the channel of their primary fluorophore. However, when tandem conjugate fluorophores degrade both the signal of the tandem conjugate fluorophore and the primary fluorophore can be present. B) P14 chimeric mice were generated by adoptive transfer of Thy1.1 P14s into Thy1.2 recipients followed by infection with LCMV-Arm. At a memory time point, mice underwent sham or CLP surgery. Day 9 post-surgery splenocytes were labeled with anti-Thy1.1-APC-efluor780. Compensation was performed for both APC-efluor780 and an empty APC channel. Representative histogram of the APC signal from APC-efluor780 labeled cells from sham (black) and CLP (red) hosts. APC GMFI [Mean: sham-179.7, CLP-624.3; standard error: sham-99.34, CLP-112.4; n: sham-3, CLP-3; $p < 0.05$: sham v CLP]. C) Utilizing the same experimental procedure as in panel B, cells were stained with the indicated antibody fluorophore and representative histograms of empty APC channel is shown. D) Splenocytes from naive mice were labeled with Thy1.2- APC-efluor780. During staining cells were exposed to normal FACs buffer or FACs buffer containing H₂O₂ (to induce oxidation). Representative histograms of empty APC channel from APC-efluor780 labeled cells exposed to either normal conditions (black) or in the presence of H₂O₂ (blue). E) Utilizing the same experimental design as in panel B, cells were labeled with anti-Thy1.1-APC-efluor780 in either the presence or absence of BME. Sham without BME (black), Sham with BME (gray), CLP without BME (red), and CLP with BME (blue). Representative histograms of empty APC channel for APC-efluor780 labeled cells are shown. APC GMFI [Mean: sham w/o BME-433.8, sham w/ BME-142.0, CLP w/o BME-1219, CLP w/o BME-933; standard error: sham w/o BME-71.79, sham w/ BME-2.72, CLP w/o BME-119.8, CLP w/o BME-228.2; n: sham w/o BME-5, sham w/ BME-5, CLP w/o BME-5, CLP w/ BME-5; $p < 0.05$: sham w/o BME v CLP w/o BME, sham w/ BME v CLP w/o BME, sham w/ BME v CLP w/ BME]. F, G) Utilizing the same experimental setup as in panel B. F) Representative gating and G) cumulative data for ROS production by splenocytes from sham (black) and CLP (red) hosts is shown. n = 5/group * = $p < 0.05$ error bars indicate standard error. H) Mice were infected IV with Plasmodium berghei ANKA (PbANKA) radiation attenuated sporozoites (RAS) followed in some mice 2 days later by IV inoculation of PyXNL infected red blood cells to generate blood-stage infection. Parasitemia was cleared by day 35 and splenocytes from both groups were harvested on day 42. Cells were labeled with anti-Thy1.2-APC-efluor780 and -CD8a-PECy7. Representative histograms for empty APC and PE channels from RAS-immunized and blood-stage infected (red) compared to RAS-immunized controls (black) for APC-efluor780 and PE-Cy7 labeled cells. APC GMFI [Mean: PbANKA RAS--379, PbANKA RAS+PyXNL iRBCs-1272; standard error: PbANKA RAS-14.94, PbANKA RAS+PyXNL iRBCs-421.6; n: PbANKA RAS-4, PbANKA RAS+PyXNL iRBCs-5; $p < 0.05$: PbANKA RAS v PbANKA RAS+PyXNL iRBCs]; PE GMFI [Mean: PbANKA RAS-23.88, PbANKA RAS+PyXNL iRBCs -163.6; standard error: PbANKA RAS-2.433, PbANKA RAS+PyXNL iRBCs-30.25; n: PbANKA RAS-4, PbANKA RAS+PyXNL iRBCs -5; $p < 0.05$: PbANKA RAS v PbANKA RAS+PyXNL iRBCs]. I) Mice were either left

naive or infected IV with 10LD50 of virulent L.m. 10403S. 2 days post-infection, spleens were harvested and stained with anti-CD8a-PE-Cy7. Representative histograms for empty PE channel from L.m. infected (red) and naive controls (black) for PE-Cy7 labeled cells. APC GMFI [Mean: Naive-179.7, L. monocytogenes-624.3; standard error: Naive -99.34, L. monocytogenes-112.4; n: Naive -3, L. monocytogenes-4; $p < 0.05$: Naive v L. monocytogenes]. J) Representative histograms and K) cumulative data for ROS production by leukocytes from healthy controls (black) and septic patients (red) is shown. $n = 10/\text{group}$ * = $p < 0.05$ error bars indicate standard error. L, M) Frozen leukocytes from septic patients and healthy controls were thawed and stained with anti-CD45-APC-Cy7. L) Representative histograms and M) cumulative GMFI data of empty APC channel on APC-Cy7-labeled cells from healthy controls (black) and septic patients (red) APC-Cy7 control (gray). $n = 10/\text{group}$ * = $p < 0.05$ error bars indicate standard error. N,O) Leukocytes were isolated from blood donation cones. Samples were split and either left at 4°C or frozen in lymphocyte freeze media. 12hrs later samples were thawed and both the samples at 4°C and the frozen samples were stained with anti-CD45-APC-Cy7. N) Representative histograms of empty APC channel on APC-Cy7 labeled cells from non-frozen cells (black) and frozen cells (red) with APC-Cy7 control (gray). O) Representative histograms for ROS production by leukocytes from the same donor blood cone that were either left at 4°C (black) or frozen (red). P) Mice were either infected with LCMV-Arm or left naive. 30 days post LCMV infection mice were split into four groups: LCMV with Sham surgery (black), LCMV infected with 1×10^7 cf.u of attenuated (ActA deficient) L.m. (gray), Naive with CLP surgery (blue), and LCMV with CLP surgery (red). 9 days after surgery or L.m. infection splenocytes were stained with anti-CD8a-APC-Cy7 and -CD11a-PE-Cy7. GMFI of APC and PE for individual samples were graphed by each other with linear regression to determine the strength of the correlation between the factors. n: LCMV +sham-4, LCMV+L.m.-4, Naive+CLP-4, LCMV+CLP-6.